

On the Acid–Base Properties of Microwave Irradiated Hydrotalcite-like Compounds Containing Zn²⁺ and Mn²⁺

Álvaro Sampieri[†] and Enrique Lima^{*·‡·§}

Colegio de Postgraduados, Campus Montecillo, Carretera México-Texcoco, km 36.5, 56230 Montecillo, Estado de México, Mexico, Instituto de Investigaciones en Materiales, Universidad Nacional Autónoma de México, Circuito exterior s/n CU, Del. Coyoacán, CP 04510 México DF, Mexico, and Universidad Autónoma Metropolitana, Iztapalapa, Av. San Rafael Atlixco No. 186 Col. Vicentina, 09340 México D.F., México

Received November 26, 2008. Revised Manuscript Received January 13, 2009

Microwave irradiated lamellar double hydroxides containing different divalent metals (Mn²⁺, Zn²⁺, or Mg²⁺) were prepared with Al³⁺ as the trivalent metal. Samples containing Mn²⁺ and Zn²⁺ were unstable at 400 °C, leading to formation of mixed oxides and spinel phases. Acid–base properties of the samples were characterized by nitromethane and CO₂ adsorption followed by FTIR spectroscopy. Decomposition of adsorbed nitromethane leads to isocyanate species that acts as probe molecules of acid–base sites at the surface. These properties determine the ability of materials to retain CO₂. Indeed, whereas Mn–O sites are able to interact directly with CO₂ molecules, Mg–O and Zn–O are able to form carbonate species as a result of the CO₂ sorption.

Introduction

Layered double hydroxides (LDHs), also known as hydroxide-like compounds,¹ are layered compounds formed by positively charged metal hydroxide sheets with intercalated anions and water molecules in the interlayer region. The chemical formula of LDHs can be expressed as [M₁²⁺_xM₃³⁺[OH]₂]^{x+}[A_{z/2}^{z-}·nH₂O]^{x-} where M²⁺ is a divalent cation (Mg²⁺, Ni²⁺, Zn²⁺, Co²⁺, Fe²⁺,...) and M³⁺ is a trivalent cation (Al³⁺, Fe³⁺, Cr³⁺,...). The positive charge of the layers is caused by the inclusion of M³⁺ cations in a neutral layer of M²⁺ cations linking by hydroxyl groups. This charge is balanced by A anions with charge z⁻, for instance, CO₃²⁻, SO₄²⁻, Cl⁻, OH⁻, or NO₃⁻, among others. Although the anions to be hosted in the interlayer space can be numerous, carbonates are, in general, preferred.² The layered structure collapses at temperatures between 200 and 400 °C due to dehydration, dehydroxylation, and decarbonation processes. Then, mixed oxides are most of times obtained, which commonly are able to recover the layered structure through contact with an anion aqueous solution. The destruction–regeneration of the layered structure is frequently referred to as “memory effect”.^{3,4} During calcination the coordination of M³⁺ ions is partially lowered from octahedral to tetrahedral. Moreover, in the rehydration step, some of the tetrahedral M³⁺ ions do not recover the octahedral coordination.^{5–7} Therefore, the physicochemical properties of the reconstructed structure became different than those of the original hydrotalcite.

LDHs are multipurpose materials that find many applications, for example, as sorbents, anion exchangers, catalysts, and catalyst precursors.⁸ The versatility of LDHs can be achieved in many ways, by either changing M²⁺, M³⁺, A^{z-} (composition and the M²⁺/M³⁺ ratio) or modifying preparation methods, for example, precipitation, sol–gel, combustion or memory effect.^{9–11} For instance, mixed oxide obtained through calcination of carbonated hydrotalcite magnesium–aluminum has been extensively used as catalyst in condensation reactions, as these catalysts exhibit strong acid–basic pairs with a predominant basicity of type Lewis. On the contrary, LDH with OH⁻ anions intercalated in the interlayer space, frequently named meixnerite, also represents a catalyst predominantly basic having Brønsted basicity and negligible acidity.¹² Mixed (Mg,Al)O oxides and meixnerite are only two examples of efficient catalysts that can be obtained from LDHs. Nevertheless, as above-mentioned the variation of metals and anion can be copious and the physicochemical properties of LDHs are then easily modulated. Hence, hydroxide-like compounds for specific tasks can be prepared. For example, mixed (Mg,Al)O oxides, containing both strong basic and strong acid sites, can be applied to deprotonate molecules and retain the corresponding anions at the surface. In contrast, in mixed (Mg,Ga)O oxides the strength of the acid sites decreases; thus, these mixed oxides are very useful in some condensation reactions.¹³ The method of preparation also influences significantly the properties of LDHs. In this sense, coprecipitation is the most recurring method to prepare hydrotalcite-like compounds containing the metal cations homogeneously distributed. However, if the variant of microwave irradiation is used in preparation of Mg–Al hydrotalcites, particles with a core enriched in

* Corresponding author. Telephone number: (525) 5804 4667. Fax number: (525) 5804 4666. E-mail address: lima@xanum.uam.mx.

[†] Colegio de Postgraduados.

[‡] Universidad Nacional Autónoma de México.

[§] Universidad Autónoma Metropolitana.

(1) Miyata, S. *Clays Clay Miner.* **1980**, *28*, 50.

(2) Miyata, S. *Clays Clay Miner.* **1983**, *31*, 305.

(3) Hibino, T.; Tsunashima, A. *Chem. Mater.* **1998**, *10*, 4055.

(4) Stanimirova, T. S.; Vergilov, I.; Kirov, G.; Petrova, N. *J. Mater. Sci.* **1999**, *34*, 4153.

(5) Stanimirova, T. S.; Kirov, G.; Donolova, E. *J. Mater. Sci. Lett.* **2001**, *20*, 453.

(6) Mackenzie, K. J.; Meinhold, R. H.; Sherriff, B. L.; Xu, Z. *J. Mater. Chem.* **1993**, *3*, 1263.

(7) Hibino, T.; Tsunashima, A. *Clays Clay Miner.* **1997**, *45*, 842.

(8) Rives, V. *Layered Double Hydroxides, present and Future*; Nova Science Ed.: New York, 2002.

(9) Valente, J. S.; Cant, M. S.; Cortez, J. G. H.; Montiel, R.; Bokhimi, X.; López-Salinas, E. *J. Phys. Chem. C* **2007**, *111*, 642.

(10) Martínez-Ortiz, M. J.; Tichit, D.; Gonzalez, P.; Coq, B. *J. Mol. Catal. A* **2003**, *201*, 199.

(11) Dávila, V.; Lima, E.; Bulbulian, S.; Bosch, P. *Microporous Mesoporous Mater.* **2008**, *107*, 240.

(12) Lima, E.; Laspéras, M.; Ménorval, L. C. D.; Tichit, D.; Fajula, F. *J. Catal.* **2004**, *223*, 28.

(13) Lima, E.; Ménorval, L.-C. D.; Tichit, D.; Laspéras, M.; Graffin, P.; Fajula, F. *J. Phys. Chem. B* **2003**, *107*, 4070.

Table 1. M^{2+}/M^{3+} Ratio and Specific Surface Area of the LDH Samples

| sample code | M^{2+} | M^{3+} | M^{2+}/M^{3+} | specific surface area ^a (m^2/g) |
|----------------|----------|----------|-----------------|--|
| Zn–Al LDH | Zn | Al | 2 | 19 |
| (Zn–Mn)–Al LDH | Zn,Mn | Al | 2 | 47 |
| Mn–Al LDH | Mn | Al | 2 | 66 |
| Mg–Al LDH | Mg | Al | 2 | 82 |

^a Determined by nitrogen isotherms and applying the BET equation.

aluminum are obtained.¹⁴ LDHs can also be modified by memory effect. This procedure is based on the capacity of mixed oxides to reconstitute the original structure upon contact with anions or simply exposure to air. The memory effect became an interesting way to produce a high number of acid sites at the surface. Furthermore, if hydrotalcites are synthesized via combustion, the particles obtained are enriched in aluminum at the external surface.¹¹

Recently it has been reported that materials with a low affinity to carbonates can be prepared by combining the coprecipitation method and microwave irradiation in the synthesis of (Mn, Zn)–Al hydrotalcites.¹⁵ The phobic carbonate character was explained in terms of the high electronegativity of Mn^{2+} ions coordinated to six oxygen ions. Such a proposition suggests that the strength of acid–base pairs is very different in these compounds, if compared to those present in the most used hydrotalcite, based on magnesium–aluminum. Of course, these materials can be claimed in adsorption and catalysis processes. To disclose the nature, diversity, and availability of acid and basic sites, we present in this work a study of probe molecule adsorption on these materials which, as a first approach, were called phobic carbonate LDHs.

Experimental Methods

Samples. Layered double hydroxides, Zn–Al and Mn–Al, with a M^{2+}/Al^{3+} molar ratio of 2/1 were synthesized by coprecipitation. Two aqueous solutions, one containing both $M^{2+}(NO_3)_2$ [with $M^{2+} = Mn^{2+}$ or Zn^{2+}] and $Al(NO_3)_3$ and the other containing NaOH (1.85 M) were simultaneously added dropwise into a flask at room temperature. The pH was not controlled during the precipitation; it varied between 7.5 and 8.5. After precipitation, samples were irradiated in a microwave reactor (MIC-I, Sistemas y Equipos de Vidrio, S. A. de C. V.) operating at 200 W for 10 min. The maximal temperature reached in the reactor was 80 °C. The precipitates were washed with deionized water and later dried at 70 °C for 24 h. To obtain the corresponding oxides, the samples were calcined at 400 °C.

The same procedure was used to prepare a ternary LDH containing (Zn–Mn)–Al, keeping the M^{2+}/M^{3+} equal to 2 [(0.2 + 1.8)/1]; Table 1.

Characterization. Samples were characterized by X-ray diffraction (XRD) and ²⁷Al nuclear magnetic resonance spectroscopy, under magic angle spinning conditions (MAS NMR) and by adsorption of CH_3NO_2 and CO_2 as infrared probe molecules. To have a reference sample, a LDH magnesium–aluminum, with a Mg^{2+}/Al^{3+} ratio of 2, prepared by coprecipitation, was also characterized.

XRD patterns were obtained with a Bruker AXS D8 advance diffractometer coupled to a copper anode X-ray tube.

²⁷Al MAS NMR spectra were acquired at a frequency of 78.15 MHz on a Bruker Avance II spectrometer. The samples were packed in ZrO_2 rotors, and they were spun at 10 kHz. Short single pulses

(14) Fetter, G.; Hernández, F.; Maubert, A. M.; Lara, V. H.; Bosch, P. J. *Porous Mater.* **1997**, *4*, 27.

(15) Sampieri, A.; Fetter, G.; Pfeiffer, H.; Bosch, P. *Solid State Sci.* **2007**, *9*, 394.

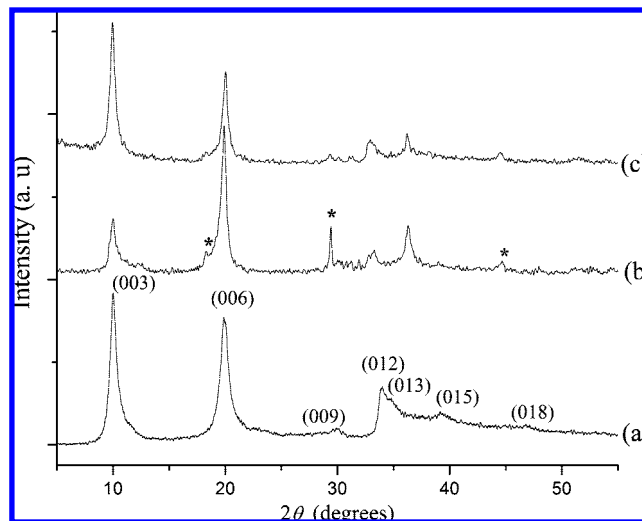


Figure 1. XRD patterns of dried samples. (a) Zn–Al LDH, (b) (Zn–Mn)–Al LDH, and (c) Mn–Al LDH. * indicates peaks due to Mn_2O_4 , and the numbers above the peaks correspond to the Miller index of hydrotalcite, JCPDS file 220700.

($\pi/12$) with a repetition time of 0.5 s were used. Chemical shifts were referenced to an aqueous 1 N $AlCl_3$ solution.

Nitromethane adsorption followed by infrared spectroscopy was performed by pressing the LDH samples and then evacuating them in a greaseless IR cell, equipped with calcium fluoride windows, connected to a vacuum line. The self-supported dried samples were outgassed at 400 °C for 8 h under 10^{-4} Torr. After activation, samples were cooled until they reached room temperature and contacted with 30 Torr of nitromethane. The excess of gas was evacuated, and the FTIR spectrum was then acquired at room temperature and 2 cm^{-1} resolution using a Perkin-Elmer FTIR 2000 spectrophotometer. To characterize the changes induced by the thermal treatment, the sample containing nitromethane was then heated under vacuum and cooled and the spectrum again recorded.

The other self-wafers were prepared and activated at 400 °C, as above explained. Then, samples were exposed to different pressures of CO_2 ; after reaching equilibrium, the excess of CO_2 was evacuated at room temperature, and the corresponding FTIR spectra were recorded.

Results

The XRD patterns of the LDHs dried at 70 °C are shown in Figure 1. They all matched with a hydrotalcite-like structure, the average d_{003} distance was 8.846 Å for the three samples; the d_{003} distance is similar to the value of nitrated LDHs. Nevertheless, a small amount of a spinel appeared in the ternary (Zn–Mn)–Al LDH attributed to the oxidation of the reactants during preparation, probably favored by the microwave irradiation.

The XRD patterns of Zn–Al and Mn–Al samples, treated at 400 °C, revealed the presence of ZnO, $ZnAl_2O_4$, and/or Mn_2O_4 and Mn_2O_3 (Figure 2). In the same way, the (Zn–Mn)–Al LDH shows a diffraction pattern indicating the formation of Mn_2O_4 and (Zn,Al) Mn_2O_4 oxides. This behavior suggests that manganese is oxidized from Mn^{2+} to Mn^{3+} and Mn^{4+} . On the contrary, the Mg–Al LDH sample with temperature follows the typical behavior leading to formation of mixed oxide $Mg(Al)O$ with periclase-like structure. Note that the XRD of the Zn–Al sample exhibits the ZnO pattern, but it must be assumed that the aluminum formed a mixed oxide with this phase since no amorphous solids were detected; that is, Zn(Al)O mixed oxide was formed.

The ²⁷Al MAS NMR spectra of the dried samples, Figure 3, show that the local environment of aluminum in the Mg–Al and Zn–Al samples differed with respect to the Mn–Al and

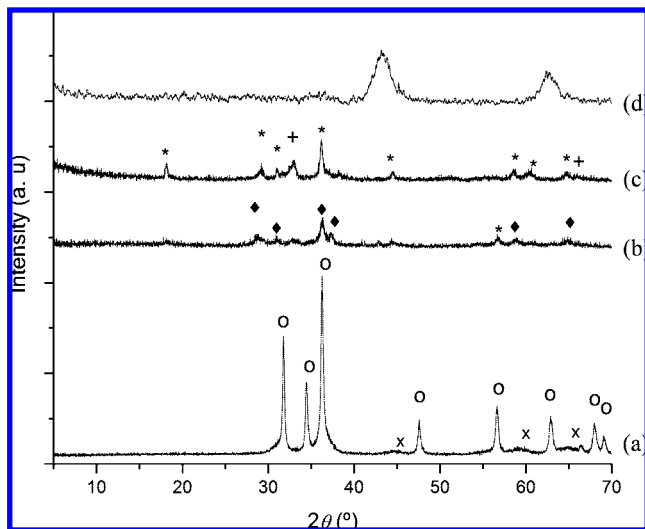


Figure 2. XRD patterns of samples treated at 400 °C. (a) Zn-Al LDH, (b) (Zn-Mn)-Al LDH, and (c) Mn-Al LDH and (d) Mg-Al LDH. Diffraction peaks are labeled as * for Mn_2O_4 , + for Mn_2O_3 , ♦ for ZnMn_2O_4 , O for ZnO, and x for ZnAl_2O_4 .

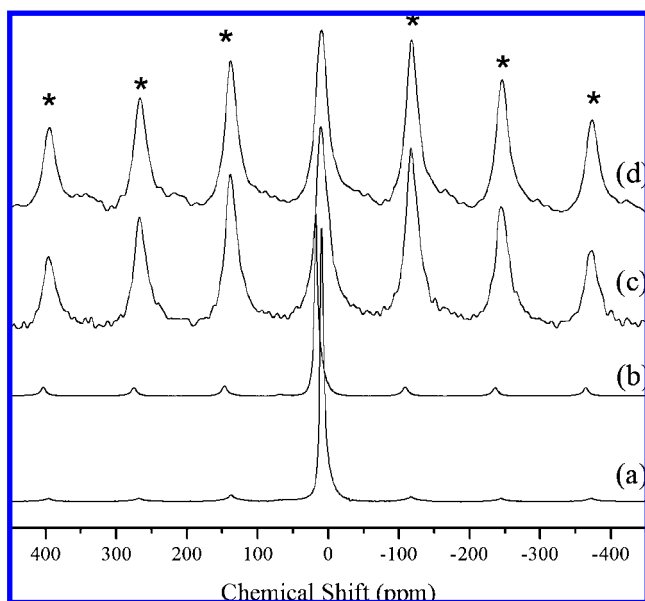


Figure 3. ^{27}Al MAS NMR spectra of (a) Mg-Al LDH, (b) Zn-Al LDH, (c) (Zn-Mn)-Al LDH, and (d) Mn-Al LDH. * indicates spinning side bands (spinning rate 10 kHz).

(Zn-Mn)-Al samples. The typical signal assigned to aluminum 6-fold coordinated in an oxygen environment (Al^{VI}) is clearly observed at ~ 0 ppm, except for the Zn-Al, where the Al^{VI} peak shifted 7 ppm toward weaker fields. For the Mn-containing sample this peak was very broad, and the anisotropy was stronger than in the other samples (Mg-Al and Zn-Al LDH).

In the case of the samples treated at 400 °C, Figure 4, remarkable differences on ^{27}Al MAS NMR spectra were observed. For instance, Mg-Al and Zn-Al spectra still show a peak at ~ 0 ppm corresponding to aluminum octahedral (Al^{VI}). Besides, a new peak appears at ~ 70 ppm, which is attributed to aluminum in tetrahedral coordination (Al^{IV}).¹⁶ In contrast, the (Zn-Mn)-Al spectrum only indicates Al^{VI} with intense spinning side bands revealing strong anisotropy. Noticeably, the spectrum of Zn-Al

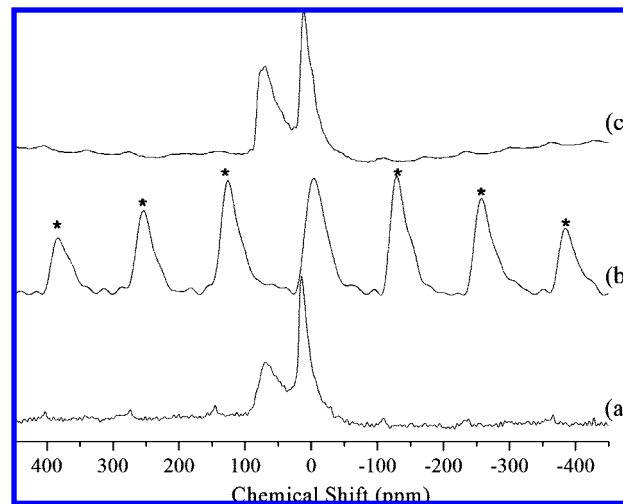


Figure 4. ^{27}Al MAS NMR spectra of (a) Mg-Al LDH, (b) (Zn-Mn)-Al LDH, and (c) Zn-Al LDH. * indicates spinning side bands (rate spinning 10 kHz).

LDH presents more contribution of Al^{IV} than the Mg-Al LDH. It is worth mentioning that the spectrum corresponding to the sample Mn-Al does not appear in the Figure 4 because of the difficulty in obtaining it: it seems that second order effect became very strong as a result of the quadrupolar character of the manganese nucleus. However, it is important to emphasize the differences evidenced in the other three samples: the ^{27}Al NMR signal intensity of 4-fold coordinated aluminum, Al^{IV} , and anisotropy vary significantly depending on the divalent cation. Of course, the variation in the $\text{Al}^{\text{IV}}/\text{Al}^{\text{VI}}$ ratio could modify structural and/or surface properties. XRD results support the appearance of oxides such as ZnAl_2O_4 , Mn_2O_3 , and ZnMn_2O_4 as a consequence of thermal treatment. The segregation of these oxides could be a profitable feature because the diversity of metal-oxygen pairs could be significantly modified. In this context, adsorption of probe molecules is a good strategy to characterize the physicochemical properties of surfaces. The goal of the present work is, then, to know the availability of these oxides to receive molecules and in such a case to elucidate the nature of the adsorption sites.

The FTIR spectra of dried samples after adsorption of nitromethane and evacuation at 25 and 110 °C are presented in Figure 5. Before adsorption, Zn-Al, Mn-Al, and (Zn-Mn)-Al samples showed spectra of surfaces almost “clean”, only a very weak absorption band ascribed to nitrate species was observed close to 1400 cm^{-1} . On the contrary, the spectrum of sample Mg-Al exhibited broad bands between 1200 and 1700 cm^{-1} before and after nitromethane adsorption, which are characteristic of the remaining carbonate species at the surface of the Mg-Al LDH.^{17,18} For the sake of conciseness, only the spectrum before adsorption of the sample Zn-Al was included as a reference spectrum (Figure 5a). After adsorption of nitromethane at 25 °C, all the samples followed the same trend in adsorbing nitromethane, either in the form of nitromethane or dissociated, that is, deprotonated and adsorbed as aci-anion nitromethane. Here it is convenient to clarify that it is necessary to specify which tautomer aci-nitromethane loses the proton to form aci-anion nitromethane. Table 2 contains the assignments of the main absorption bands.

(17) Yamaguchi, M. *J. Chem. Soc., Faraday Trans.* **1997**, 93, 3581.

(18) Nesterenko, N.; Lima, E.; Graffin, P.; Ménorval, L. D.; Laspéras, M.; Ticht, D.; Fajula, F. *New J. Chem.* **1999**, 23, 665.

(16) Samoson, A.; Lippmaa, E.; Engelhardt, G.; Lohse, U.; Jerschewitz, H. *J. Chem. Phys. Lett.* **1987**, 134, 589.

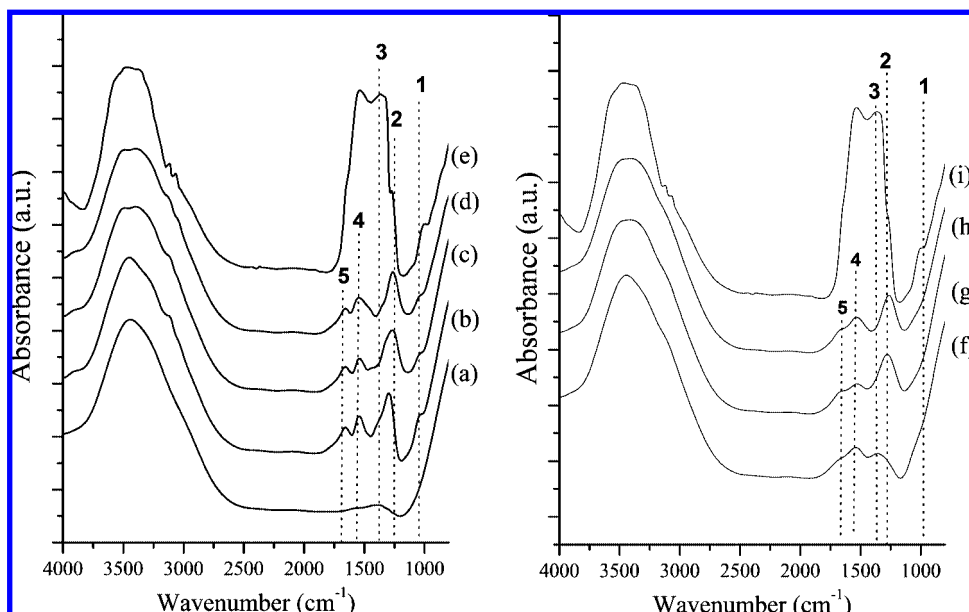


Figure 5. FTIR spectra of samples activated under vacuum at 400 °C and after adsorption of CH_3NO_2 and subsequent desorption at 25 °C (left) or 110 °C (right). (b and f) Zn–Al LDH, (c and g) (Zn–Mn)–Al LDH, (d and h) Mn–Al LDH, and (e and i) Mg–Al LDH. Spectrum (a) corresponds to sample Zn–Al LDH before CH_3NO_2 .

Table 2. Assignment^a of Absorption Infrared Bands of Nitromethane Adsorbed on LDH samples

| numbering band ^b | wave number (cm^{-1}) | species | assignment |
|-----------------------------|----------------------------------|------------------------|--------------------------|
| 1 | 1033 | aci-anion nitromethane | $\nu_a(\text{NO}_2)$ |
| 2 | 1272 | aci-anion nitromethane | $\nu_a(\text{NO})$ |
| 3 | 1375 | nitromethane | $\delta_s(\text{CH}_3)$ |
| 4 | 1565 | nitromethane | $\nu(\text{NO}_2)$ |
| 5 | 1660 | aci-anion nitromethane | $\nu(\text{C}=\text{N})$ |

^a According to refs 17–19. ^b Figure 5.

The largest net difference among the sets of spectra is that after outgassing nitromethane at 110 °C, the bands close to 1660 and 1275 cm^{-1} , which are attributed to aci-anion nitromethane, were almost absent in the sample Zn–Al LDH, Figure 5f. This result suggests the absence of strong acid to stabilize the aci-anion. All the other samples presented the band due to aci-anion nitromethane as well-defined and intense, Figure 5g–i.

Figure 6 displays the FTIR spectra series of samples Zn–Al LDH and Mn–Al LDH activated at 400 °C, after adsorption of nitromethane and consequent evacuation at different temperatures. As expected, anionic and covalently isocyanate species (bands between 2200 and 2270 cm^{-1}) were bonded at the surface of the solids as a consequence of thermal decomposition of nitromethane.¹⁹ Several remarks have to be enunciated.

(1) At temperatures as high as 200 °C, a significant amount of aci-anion nitromethane remained on the solid containing only manganese as divalent metal, Mn–Al. In other words, the reaction toward isocyanates was partially inhibited in this case. In contrast, in the other samples, isocyanate species (NCO , NCO^-) were detected at any temperature (150–400 °C)

(2) The solid containing only Zn^{2+} as divalent metal presented the less intense band due to isocyanates which were almost completely desorbed at temperatures as low as 350 °C.

(3) The position of the infrared absorption bands of isocyanate species was found to be highly linked to the composition of

solids. The characteristic absorption bands ranging from 2190 to 2220 cm^{-1} and 2225 to 2270 cm^{-1} are associated to isocyanate species bonded anionically and covalently, respectively (Table 3).

Figure 7 presents the isotherms of CO_2 at 25 °C onto various samples previously activated under vacuum at 400 °C. Significant differences were observed. For instance, the Mg–Al sample uptakes the highest amount of CO_2 (0.30 mmol/g), while the lowest amount (0.10 mmol/g) was detected for the Zn–Al LDH. Furthermore, the samples containing Zn^{2+} , Zn–Al, and (Zn–Mn)–Al reached the “plateau” at lower pressure than the Mg–Al and Mn–Al samples.

Figure 8 displays the FTIR spectra recorded on the samples after CO_2 adsorption at low (50 Torr) and high pressures (250 Torr). Samples behaved differently regarding the nature of the species stabilized. The absorption bands revealed three different forms of CO_2 sorption in both samples: (1) CO_2 physisorbed on the solid surface (bands between 2340 and 2365 cm^{-1}), (2) CO_2 molecules strongly interacting with metal–oxygen sites to stabilize carbonate species (bands near to 1670 and 1450 cm^{-1}), and (3) free anions, CO_3^{2-} (characteristic band close to 1360 cm^{-1}).^{20–22} At low CO_2 pressure, free carbonate anions were almost undetected in the samples containing Mn, although at high pressure, carbonate species were evident only in the (Zn–Mn)–Al LDH sample. In the case of the Mg–Al sample, it was difficult to disclose if the absorption bands of carbonate were favored as a consequence of the CO_2 sorption since before the adsorption the large bands were observed in the concerning spectral window.

Discussion

LDHs containing Mn–Al, Zn–Al, or Zn–Mn–Al have very different acidic and basic sites than those found in the reference sample Mg–Al. These differences are relating to the electronegativity of metals M^{2+} . Besides, ZnAl_2O_4 and $(\text{Zn},\text{Al})\text{Mn}_2\text{O}_4$ are formed at lower temperature than the MgAl_2O_4 . This feature is at the origin of the instability of the LDHs containing Mn or Zn

(19) Ukisu, Y.; Sato, S.; Muramatsu, G.; Yoshida, K. *Catal. Lett.* **1991**, *11*, 177.

(20) Yagi, F.; Tsuji, H.; Hattori, H. *Microporous Mater.* **1997**, *9*, 237.

(21) Lavalley, J. C. *Catal. Today* **1996**, *27*, 377.

(22) Dösköcil, E. J.; Davis, R. J. *J. Catal.* **1999**, *188*, 353.

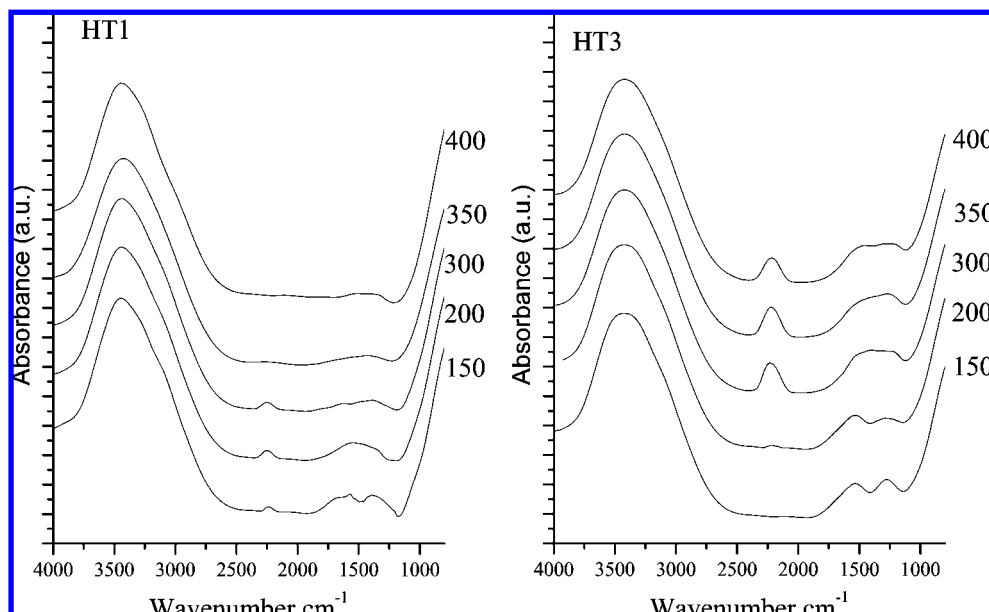


Figure 6. FTIR spectra of samples Zn–Al LDH and Mn–Al LDH after adsorption of nitromethane and subsequent evacuation at the temperature indicated in degrees celsius.

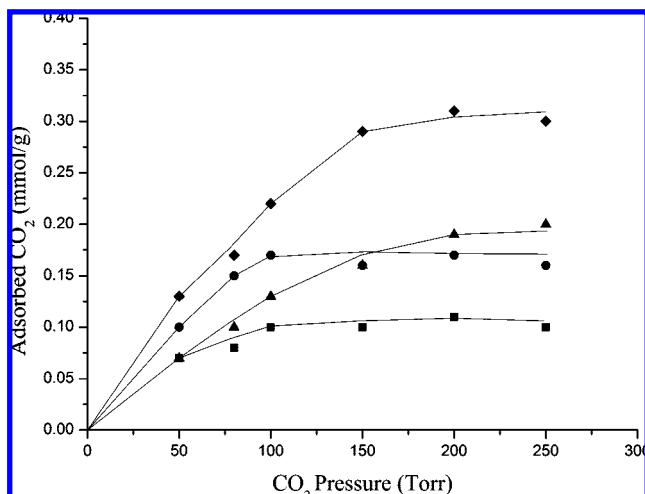


Figure 7. Adsorption capacity of carbon dioxide at 25 °C on samples previously treated under vacuum at 400 °C. Zn–Al LDH (■), (Zn–Mn)–Al LDH (●), Mn–Al LDH (▲), and Mg–Al LDH (◆).

Table 3. Position of Infrared Absorption Bands of Isocyanates Adsorbed in the Various Samples

| sample | position of infrared absorption band (cm ⁻¹) | |
|----------------|--|------------------|
| | NCO | NCO ⁻ |
| Zn–Al LDH | 2258 | 2211 |
| (Zn–Mn)–Al LDH | 2241 | 2201 |
| Mn–Al LDH | 2252 | 2208 |
| Mg–Al LDH | 2233 | 2191 |

upon the microwave irradiation. As a consequence of phase segregation, aluminum with low coordination (4-fold) occurs. The Al^{IV} formation is favored if Zn is the unique divalent metal in the Zn–Al LDH precursor. However, if Zn and Mn are present simultaneously as the divalent metals, aluminum is incorporated to the structure of the mixed compounds as 6-fold coordinated, inhibiting the creation of Al^{IV} centers. The segregation of Zn-enriched and Mn-enriched oxides is not at all negative because of the promotion of dissimilar physicochemical properties at surfaces of various composite materials, obtained from the thermal

treatment of LDHs. Indeed, the increasing of the content of Al^{IV} in the calcined Zn–Al LDH (if compared with the calcined Mg–Al LDH) could be favorable to catalysis of reactions where acid sites of moderated strength are claimed. Furthermore, the variety of acid–base pairs is significantly influenced as Zn or Mn is included in the LDH precursor. Note, for example, the extremely different behavior of nitromethane adsorbed in the various samples. The strength of interaction between the CH₃NO₂ molecule and the composite surface is determined by the nature of available oxygen–metal sites. The absence of aci-anion nitromethane on the Zn–Al LDH does not necessarily imply that it is not produced. On the contrary, because of low pK_a of aci-nitromethane, surely the anions were produced but they were not stabilized as result of absence of strong sites on the surface of this material. Instead, these species could adsorb weakly on the Zn–O sites, but they are released with temperature. Although NMR reveals the formation of an important amount of Al^{IV}, the acid sites (like Al–O) could be into the structure of the spinel-like structures; hence, these sites are not available.

The position of the infrared absorption band of isocyanate species was previously related to the nature of the surface,^{23,24} particularly to the strength of acid–base pairs in mixed oxides: the higher acid on the surface of the solid,¹⁸ the higher the wavenumber of the band. If this trend is assumed in our samples, the strength of basic sites in the LDHs increases as follows: Mg–Al > (Zn–Mn)–Al > Mn–Al > Zn–Al. Therefore, the inclusion of Zn and Mn into LDHs contributes to decreasing the basicity and increasing the acidity in the LDHs. This fact could be explained by the difference of electronegativities among the metal ions M²⁺ involved in various LDHs. Camacho-Rodrigues applied a modified Sanderson electronegativity model²⁵ to calculate the local electronegativity in hydroxalite-like compounds with various M²⁺ metals and Al³⁺ as the trivalent cation. Such a model defines the local electronegativity (S_i) as follows: S_i = [((S_{M²⁺})(S_O))^{0.5P}((S_{Al³⁺})(S_O³⁻))^{0.2Q}]^{1/6} where P and Q are integers and their sum is equal to 6 since the model considers

(23) Radtke, F.; Koeppl, R. A.; Minardi, E. G.; Baiker, A. *J. Catal.* **1997**, *167*, 127.

(24) Salama, T. M.; Ohnishi, R.; Shido, T.; Ichikawa, M. *J. Catal.* **1996**, *162*, 169.

(25) Camacho-Rodrigues, A. C. *J. Math. Chem.* **2005**, *37*, 347.

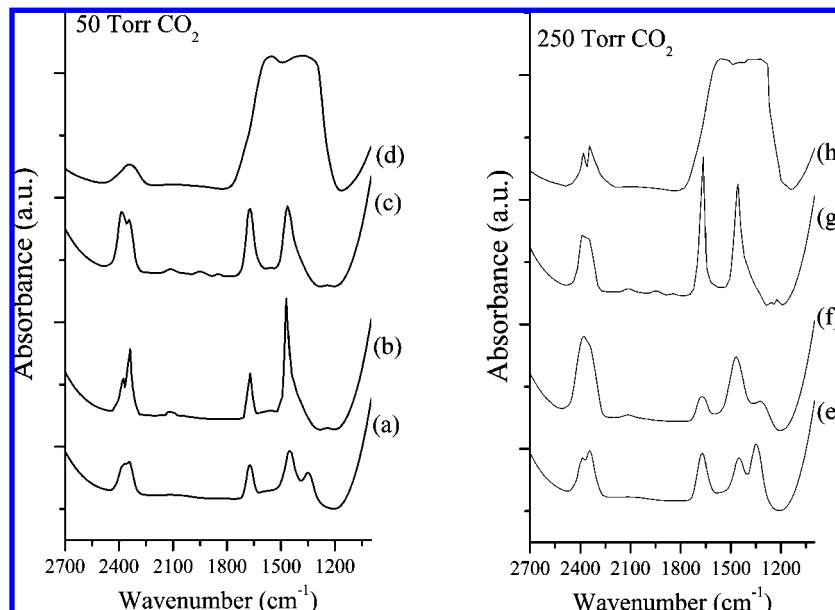


Figure 8. FTIR spectra of samples after outgassing at 400 °C and adsorption of CO₂ at 25 °C with a pressure of CO₂ of 50 and 250 Torr. (a and e) Zn–Al LDH, (b and f) (Zn–Mn)–Al LDH, (c and g) Mn–Al LDH, and (d and h) Mg–Al LDH.

the environment of the ions to be octahedral; $S_{M^{2+}}$, $S_{Al^{3+}}$, and S_O are the Sanderson's electronegativity value of atoms M^{2+} , Al^{3+} , and oxygen, respectively. The model allows the calculation of the partial charge of oxygen. In a series where the trivalent cation is constant and the M^{2+} varies, the solid became more basic if the absolute hardness²⁶ of divalent cation augments. From this trend and taking into account the absolute hardness of Zn^{2+} , Mg^{2+} , and Mn^{2+} ,^{27–29} our sample series should be classed from high to low basicity as Mg–Al > Zn–Al > (Zn–Mn)–Al > Mn–Al which does not match with the trend found with the nitromethane adsorption. In fact, only the sample Zn–Al behaves differently experimentally than the model predicts. Nevertheless it should be considered that in the Zn–Al LDH sample the highest intensity of the NMR signal of Al^{IV} was found. Then, a large amount of unsaturated aluminum is present and contributes to acidity of the solid. In consequence, the strength of the base site is lower in the Zn containing sample than the Mg and Mn containing samples.

Of course, the physicochemical properties discussed above for various samples are determinant in the CO₂ adsorption, Figure 7. For example, the LDHs containing Zn present Zn–O pairs where CO₂ interacts with the surface and leads to formation of carbonate species:



These carbonate species are stabilized coating the material's surface and making difficult the CO₂ diffusion into deeper sites. Thus, the “plateau” in Zn-containing samples is reached at lower

pressure than in samples Mg–Al and Mn–Al. On the contrary, in these latest samples most probably a dynamic adsorption–desorption mechanism is established, leading to adsorptions of CO₂ at higher pressure.

In the case of the Mn–Al LDH, the Mn–O and Al–O pairs appear as the main adsorption sites of CO₂; thus, the formation of carbonate species is inhibited. Indeed, these solids exhibit adsorption sites stronger than those of Zn– or Mg–Al LDHs, as confirmed by nitromethane adsorption. These facts explain that Zn–Al and Mg–Al mixed oxides recovered the layered structure of LDHs through memory effect but, in the samples containing manganese, such regeneration does not occur.

Conclusion

Acid–base properties of M^{2+} -AlLDHs can be easily modulated modifying their composition by incorporation of several M^{2+} metals with different electronegativities. If Mn^{2+} and Zn^{2+} are used, the LDHs became unstable at 400 °C as materials emerged are composed of oxides and spinels. The acid–base properties of the Mn–Al and Zn–Al materials are very different from those of mixed oxide (Mg,Al)O, obtained through calcination of Mg–Al LDH precursor. Indeed, Mn^{2+} induces the formation of strong Mn–O sites that retain CO₂ without formation of carbonate species, avoiding the layer reconstruction through memory effect, commonly observed in the classic Mg–Al LDH. On the contrary, the presence of Zn–O pairs is suitable to sequester CO₂ and also to form carbonate species, favoring the reconstruction of Zn–Al LDH through the memory effect.

Acknowledgment. Thanks are due to Conacyt for financial support, Grant 24676.

LA803920C

(26) Parr, R. G.; Pearson, R. G. *J. Am. Chem. Soc.* **1983**, *105*, 6801.

(27) Pearson, R. G. *Inorg. Chem.* **1988**, *27*, 734.

(28) Sanderson, R. T. *J. Am. Chem. Soc.* **1983**, *105*, 2259.

(29) Sanderson, R. T. *Inorg. Chem.* **1986**, *25*, 3518.